SIAM J. SCI. COMPUT.
Vol. 30, No. 5, pp. 2263–2285

A NUMERICAL METHOD FOR THE GENERALIZED REGULARIZED LONG WAVE EQUATION USING A REPRODUCING KERNEL FUNCTION*

SHUSEN XIE†, SEOKCHAN KIM‡, GYUNGSOO WOO‡, AND SUCHEOL YI‡

Abstract. A new numerical method for solving the generalized regularized long wave equation is devised and analyzed. By using a reproducing kernel function, the numerical solution at each discrete time step is obtained by an explicit integral expression even though the scheme is truly implicit, and, hence, the computation is fully parallel. The error estimates are given and some numerical results are presented.

Key words. generalized regularized long wave equation, reproducing kernel function, solitary wave

AMS subject classifications. 35A40, 65M99

DOI. 10.1137/070683623

1. Introduction.

The generalized regularized long wave (GRLW) equation can be written as

$$u_t + \alpha u_x + \beta u u_x - \mu u_{xx} - \delta u_{xxt} = 0, \tag{1.1}$$

where the subscripts t and x denote differentiation and α, β, μ, and δ are nonnegative constants. In accordance with the different values of constants α, β, μ, and δ, (1.1) includes some special equations such as the equal width equation for $\alpha = \mu = 0$, $\beta = 1$, and $\delta \neq 0$ and the regularized long wave (RLW) equation for $\alpha = 1$, $\beta \neq 0$, $\delta \neq 0$, and $\mu = 0$.

Peregrine [17] originally introduced the RLW equation as an alternative to the KdV equation to study soliton phenomena and as a model for small amplitude long waves on the surface of water. This equation also has been used to model a variety of phenomena such as nonlinear transverse waves in shallow water, ion-acoustic and magnetohydrodynamic waves in plasma, and phonon packets in nonlinear crystals. Analytical solutions of the RLW equation can be found for the limited initial and boundary conditions, and, hence, numerical solutions of the RLW equation are very useful to study some of the physical phenomena. Various numerical techniques such as the finite difference methods [2, 10, 11, 15, 18], the spectral method [14], and the finite element, B-spline finite element, and least-squares finite element methods [4, 5, 9, 12, 13, 21, 22] have been devised to find numerical solutions of the RLW equation.

In this paper, a numerical method using a reproducing kernel function is developed to solve the GRLW equation numerically. We consider the following initial and

*Received by the editors February 25, 2007; accepted for publication (in revised form) February 11, 2008; published electronically June 11, 2008.
http://www.siam.org/journals/sisc/30-5/68362.html

†Department of Mathematics, Ocean University of China, Qingdao, 266071 People's Republic of China (shusenxie@ouc.edu.cn). This author's work was supported by the National Natural Science Foundation of China (40276008).

‡Department of Applied Mathematics, Changwon National University, Changwon, 641-773, Republic of Korea (sckim@changwon.ac.kr, gswoo@changwon.ac.kr, scyi@changwon.ac.kr). The work of these authors was supported by Changwon National University in 2006.

boundary value problem:

$$\begin{aligned} u_t + \alpha u_x + \beta u u_x - \mu u_{xx} - \delta u_{xxt} = 0, &\quad (x,t) \in I \times (0,T], \\ u(a,t) = u(b,t) = 0, &\quad t \in (0,T], \\ u(x,0) = u_0(x), &\quad x \in I, \end{aligned} \tag{1.2}$$

where δ is a positive constant.

Boundary conditions $u(a,t) = u(b,t) = 0$ are used to model the physical condition that solution u tends to zero as $|x|$ gets larger. For most of the problems considered, the initial data $u_0(x)$ are usually a localized smooth function (solitary wave) which decreases exponentially as $|x|$ tends to infinity. So the interval $I = (a,\ b)$ may be chosen long enough so that the boundaries do not affect the wave interactions during a finite time period $[0,T]$. Physical problems with nonhomogeneous Dirichlet, periodic, or Neumann boundary conditions (e.g., undular bore [2, 9, 21] and periodic orbits [6]) can also be treated for a long enough finite interval I.

We will formulate our time discrete approximation based on the variational form of problem (1.2). By using a reproducing kernel function for the test function, the numerical solution at each discrete time level is obtained by an explicit integral expression even though the scheme is implicit, and so the computation is fully parallel. In this approach, finding a reproducing kernel function is a crucial step in solving a given boundary condition problem. The nonhomogeneous Dirichlet, periodic, or Neumann boundary conditions can be dealt with by reproducing kernel functions, and suitable reproducing kernel functions for these kinds of boundary condition problems can be found.

In section 2, some numerical schemes are formulated by means of a reproducing kernel function. Error estimates are given in section 3. Some numerical results are presented in section 4.

2. Numerical schemes. Let $H^m := H^m(I)$ and $H_0^m := H_0^m(I)$ denote the Sobolev spaces, where m is a positive integer, and let $(\cdot,\cdot)$ denote the usual inner product on $L_2(I)$. The equivalent variational form of problem (1.2) can be written as follows.

Find $u(\cdot,t) \mid (0,T] \to H_0^1$ such that

$$\begin{aligned} &(u_t, v) + \alpha(u_x, v) + \beta(u u_x, v) + \mu(u_x, v_x) + \delta(u_{xt}, v_x) = 0 \quad \forall v \in H_0^1, \\ &u(x,0) = u_0(x). \end{aligned} \tag{2.1}$$

In this section, we consider two schemes of a semidiscrete approximation in time variable. The full-discrete approximations follow directly from the semidiscrete ones.

2.1. The first-order accurate semidiscrete approximation. Let Δt denote the time step, $t^n = n\Delta t$, and $u^n(x) = u(x,t^n)$ for $n = 0,1,\ldots,N := T/\Delta t$. For simplicity we also use notations $\partial_t u^n$ and $\bar{\partial}_t u^n$ for difference quotients, i.e., $\partial_t u^n := (u^{n+1} - u^n)/\Delta t$ and $\bar{\partial}_t u^n := (u^{n+1} - u^{n-1})/(2\Delta t)$.

The first-order accurate semidiscrete approximation in time variable can be defined as follows.

Scheme 1. Find $U^{n+1} \in H_0^1$ for $n = 0,1,\ldots,N-1$ such that

$$\begin{aligned} &(\partial_t U^n, v) + \delta\,(\partial_t U_x^n, v_x) \\ &= -\alpha(U_x^n, v) - \beta(U^n U_x^n, v) - \mu(U_x^n, v_x) \quad \forall v \in H_0^1, \end{aligned} \tag{2.2}$$

where $U^0 = u_0$.

We will consider the explicit expression for the solution to (2.2) by using a reproducing kernel function. Let W_0^δ denote the set of all functions in H_0^1 equipped with an inner product

$$\langle u,\ v\rangle = \int_a^b (uv + \delta u_x v_x)\ dx,$$

and the associated norm is defined by $\|\cdot\|_{W_0^\delta} = \sqrt{\langle\cdot,\cdot\rangle}$. Then the space W_0^δ is a Hilbert space, since the two norms $\|\cdot\|_{W_0^\delta}$ and $\|\cdot\|_{H^1}$ are equivalent.

For every $y \in [a,b]$ we define a mapping $\mathcal{F}^y : W_0^\delta \longrightarrow \Re$ by

$$\mathcal{F}^y(v) = v(y) \quad \forall v \in W_0^\delta.$$

Then it can be easily shown that $\mathcal{F}^y$ is a bounded linear functional on W_0^δ. By the Riesz representation theorem there exists a unique function $R^y \in W_0^\delta$, which depends on y, such that

$$\mathcal{F}^y(v) = v(y) = \langle v,\ R^y\rangle \quad \forall v \in W_0^\delta. \tag{2.3}$$

We introduce the analytical representation of R^y. Consider the following boundary value problem with y as a parameter:

$$\begin{aligned}
&\delta\frac{d^2}{dx^2}R^y(x) - R^y(x) = 0, \quad x \neq y;\\
&R^y(x)|_{x=y-0} = R^y(x)|_{x=y+0};\\
&\frac{d}{dx}R^y(x)|_{x=y-0} - \frac{d}{dx}R^y(x)|_{x=y+0} = \frac{1}{\delta};\\
&R^y(x)|_{x=a} = R^y(x)|_{x=b} = 0.
\end{aligned} \tag{2.4}$$

It can be shown that the solution of problem (2.4) is

$$R^y(x) = \frac{\sinh\frac{b-\max(x,y)}{\sqrt{\delta}}\sinh\frac{\min(x,y)-a}{\sqrt{\delta}}}{\sqrt{\delta}\sinh\frac{b-a}{\sqrt{\delta}}}, \quad (x,y) \in I \times I. \tag{2.5}$$

It is easy to verify that the function R^y in (2.5) satisfies (2.3). We call R^y the reproducing kernel function (RKF) of W_0^δ [1, 20].

Remark. Analytical representation of the RKF for a general Hilbert space $(H, \langle .,.\rangle)$ is usually unknown. The RKF depends on the boundary conditions of functions in H and the inner product $\langle\cdot,\cdot\rangle$. Let $\{\psi_i(x)\}_{i=1}^\infty$ denote the orthonormal basis for H, that is, $\langle\psi_i(x),\psi_j(x)\rangle = \delta_{ij}$, where δ_{ij} is the Kronecker δ, defined by $\delta_{ij} = 0$ if $i \neq j$ and $\delta_{ij} = 1$ if $i = j$. Then the RKF $R^y(x)$ for H can be constructed formally as

$$R^y(x) = \sum_{j=1}^\infty \psi_j(x)\psi_j(y).$$

With the inner product $\langle\cdot,\cdot\rangle$, (2.2) can be rewritten as

$$\begin{aligned}
\langle\partial_t U^n, v\rangle &= -\alpha(U_x^n, v) - \beta(U^n U_x^n, v) - \mu(U_x^n, v_x)\\
&= -\alpha(U_x^n, v) - \beta(U^n U_x^n, v) - \frac{\mu}{\delta}\langle U^n, v\rangle + \frac{\mu}{\delta}(U^n, v) \quad \forall v \in H_0^1.
\end{aligned} \tag{2.6}$$

For each $y \in [a,\ b]$ we know that $R^y \in H_0^1$. By taking $v(x) = R^y(x) =: R(x,y)$ in (2.6), we obtain

$$U^{n+1}(y) = \left(1 - \frac{\mu}{\delta}\Delta t\right) U^n(y) - \Delta t \int_a^b \left\{\alpha U_x^n(x) - \frac{\mu}{\delta} U^n(x)\right\} R(x,y)\ dx$$

$$- \beta \Delta t \int_a^b U^n(x) U_x^n(x) R(x,y)\ dx \quad \forall y \in [a,b]. \tag{2.7}$$

Then (2.7) gives an explicit expression of the solution to (2.2).

It follows from (2.7) that the derivative of the approximate solution is

$$U_y^{n+1}(y) = \left(1 - \frac{\mu}{\delta}\Delta t\right) U_y^n(y) - \Delta t \int_a^b \left\{\alpha U_x^n(x) - \frac{\mu}{\delta} U^n(x)\right\} R_y(x,y)\ dx$$

$$- \beta \Delta t \int_a^b U^n(x) U_x^n(x) R_y(x,y)\ dx \quad \forall y \in [a,b]. \tag{2.8}$$

2.2. The second-order accurate semidiscrete approximation. We now give a second-order accurate semidiscrete approximation in time variable.

Scheme 2. Find $U^{n+1} \in H_0^1$ for $n = 1, \ldots, N-1$ such that

$$\begin{aligned} &\left(\bar{\partial}_t U^n, v\right) + \delta \left(\bar{\partial}_t U_x^n, v_x\right) \\ &= -\alpha(U_x^n, v) - \beta(U^n U_x^n, v) - \mu(U_x^n, v_x) \quad \forall v \in H_0^1, \\ &\left(\partial_t U^0, v\right) + \delta \left(\partial_t U_x^0, v_x\right) = -\alpha(U_x^0, v) - \beta(U^0 U_x^0, v) - \mu(U_x^0, v_x), \end{aligned} \tag{2.9}$$

where $U^0 = u_0$.

By means of the inner product $\langle \cdot, \cdot \rangle$, the equations in scheme 2 can be rewritten as

$$\begin{aligned} \langle \bar{\partial}_t U^n, v\rangle &= -\alpha(U_x^n, v) - \beta(U^n U_x^n, v) - \mu(U_x^n, v_x), \\ \langle \partial_t U^0, v\rangle &= -\alpha(U_x^0, v) - \beta(U^0 U_x^0, v) - \mu(U_x^0, v_x). \end{aligned}$$

By taking $v(x) = R^y(x)$, we obtain

$$\begin{aligned} U^{n+1}(y) = U^{n-1}(y) &- \frac{2\mu}{\delta}\Delta t U^n(y) \\ &- 2\Delta t \int_a^b \left\{\alpha U_x^n(x) - \frac{\mu}{\delta} U^n(x)\right\} R(x,y)\ dx \\ &- 2\beta \Delta t \int_a^b U^n(x) U_x^n(x) R(x,y)\ dx \quad \forall y \in [a,b] \end{aligned} \tag{2.10}$$

and

$$U^1(y) = \left(1 - \frac{\mu}{\delta}\Delta t\right) U^0(y) - \Delta t \int_a^b \left\{\alpha U_x^0(x) - \frac{\mu}{\delta} U^0(x)\right\} R(x,y)\ dx$$

$$- \beta \Delta t \int_a^b U^0(x) U_x^0(x) R(x,y)\ dx \quad \forall y \in [a,b]. \tag{2.11}$$

The derivatives of approximate solutions U^{n+1} and U^1 in (2.10) and (2.11) are given as

$$\begin{aligned} U_y^{n+1}(y) = U_y^{n-1}(y) &- \frac{2\mu}{\delta}\Delta t U_y^n(y) \\ &- 2\Delta t \int_a^b \left\{\alpha U_x^n(x) - \frac{\mu}{\delta}U^n(x)\right\} R_y(x,y)\ dx \\ &- 2\beta\Delta t \int_a^b U^n(x)U_x^n(x)R_y(x,y)\ dx \quad \forall y \in [a,b] \end{aligned}$$

and

$$\begin{aligned} U_y^1(y) = \left(1 - \frac{\mu}{\delta}\Delta t\right) U_y^0(y) &- \Delta t \int_a^b \left\{\alpha U_x^0(x) - \frac{\mu}{\delta}U^0(x)\right\} R_y(x,y)\ dx \\ &- \beta\Delta t \int_a^b U^0(x)U_x^0(x)R_y(x,y)\ dx \quad \forall y \in [a,b]. \end{aligned}$$

2.3. Full-discrete approximations. In this subsection, we consider the first- and second-order accurate full-discrete approximations. It follows from the Galerkin approximation that the approximate solutions can be obtained by solving an implicit algebraic system. The approximate solutions can also be computed by using explicit formulas that are derived from an RKF.

Suppose that S_h is a finite element subspace of H_0^1 based on a family of subdivision with parameter h. If $U_h^0 = \mathcal{I}_h u_0$, where $\mathcal{I}_h$ is the interpolation operator onto S_h, then the full-discrete approximations are defined as follows:

Scheme 3. Find $U_h^{n+1} \in S_h$ for $n = 0, 1, \ldots, N-1$ such that

$$\begin{aligned} U_h^{n+1}(y) = \left(1 - \frac{\mu}{\delta}\Delta t\right) U_h^n(y) &- \Delta t \int_a^b \left\{\alpha (U_h)_x^n(x) - \frac{\mu}{\delta}U_h^n(x)\right\} R(x,y)\ dx \\ &- \beta\Delta t \int_a^b U_h^n(x)(U_h)_x^n(x)R(x,y)\ dx \quad \forall y \in [a,b]. \end{aligned} \tag{2.12}$$

The derivative of approximate solution U_h^{n+1} in (2.12) is given by

$$\begin{aligned} (U_h)_y^{n+1}(y) = \left(1 - \frac{\mu}{\delta}\Delta t\right) &(U_h)_y^n(y) \\ &- \Delta t \int_a^b \left\{\alpha (U_h)_x^n(x) - \frac{\mu}{\delta}U_h^n(x)\right\} R_y(x,y)\ dx \\ &- \beta\Delta t \int_a^b U_h^n(x)(U_h)_x^n(x)R_y(x,y)\ dx \quad \forall y \in [a,b]. \end{aligned}$$

Scheme 4. Find $U_h^{n+1} \in S_h$ for $n = 1, \ldots, N-1$ such that

$$\begin{aligned} U_h^{n+1}(y) = U_h^{n-1}(y) &- \Delta t \frac{2\mu}{\delta}U_h^n(y) \\ &- 2\Delta t \int_a^b \left\{\alpha (U_h)_x^n(x) - \frac{\mu}{\delta}U_h^n(x)\right\} R(x,y)\ dx \\ &- 2\beta\Delta t \int_a^b U_h^n(x)(U_h)_x^n(x)R(x,y)\ dx \quad \forall y \in [a,b] \end{aligned} \tag{2.13}$$

and

$$U_h^1(y) = \left(1 - \Delta t\frac{\mu}{\delta}\right) U_h^0(y) - \Delta t \int_a^b \left\{\alpha(U_h)_x^0(x) - \frac{\mu}{\delta}U_h^0(x)\right\} R(x,y)\ dx$$

$$- \beta\Delta t \int_a^b U_h^0(x)(U_h)_x^0(x)R(x,y)\ dx \quad \forall y \in [a,b]. \tag{2.14}$$

The derivatives of functions U_h^{n+1} and U_h^1 in (2.13) and (2.14) can be written as

$$(U_h)_y^{n+1}(y) = (U_h)_y^{n-1}(y) - \Delta t\frac{2\mu}{\delta}(U_h)_y^n(y)$$
$$- 2\Delta t \int_a^b \left\{\alpha(U_h)_x^n(x) - \frac{\mu}{\delta}U_h^n(x)\right\} R_y(x,y)\ dx$$
$$- 2\beta\Delta t \int_a^b U_h^n(x)(U_h)_x^n(x)R_y(x,y)\ dx \quad \forall y \in [a,b]$$

and

$$(U_h)_y^1(y) = \left(1 - \Delta t\frac{\mu}{\delta}\right) (U_h)_y^0(y) - \Delta t \int_a^b \left\{\alpha(U_h)_x^0(x) - \frac{\mu}{\delta}U_h^0(x)\right\} R_y(x,y)\ dx$$
$$- \beta\Delta t \int_a^b U_h^0(x)(U_h)_x^0(x)R_y(x,y)\ dx \quad \forall y \in [a,b].$$

3. Convergence analysis. Throughout this section, the symbol M denotes a generic positive constant not necessarily the same at different occurrences. Let $\|\cdot\|_{W_q^m}$ and $\|\cdot\|_{H^s}$ denote the norms of Sobolev spaces $W_q^m := W_q^m(I)$ and $H^s := H^s(I)$, respectively. We assume that the finite element space S_h satisfies the following approximation property:

$$\|w - \mathcal{I}_h w\|_{W_q^m} \le Mh^{r-m}\|w\|_{W_q^r} \quad \forall w \in W_q^r(I), \quad 1 \le q \le \infty, \quad m = 0, 1.$$

By the definition of $R(x,y)$ we have

$$R(x,y) := R^y(x) = R^x(y) =: R(y,x) \ge 0 \quad \forall x, y \in [a,b],$$

and it can be shown that RKF R^y has the following properties:

$$0 \le \int_a^b R(x,y)\ dx = 1 - \frac{\cosh\frac{b+a-2y}{2\sqrt{\delta}}}{\cosh\frac{b-a}{2\sqrt{\delta}}} < 1;$$

$$\left(\int_a^b (R(x,y))^2\ dx\right)^{1/2} \le \frac{1}{2\sqrt[4]{\delta}}\sqrt{\tanh\frac{b-a}{2\sqrt{\delta}}} < \frac{1}{2\sqrt[4]{\delta}} =: M_1;$$

$$\int_a^b \left|\frac{\partial R(x,y)}{\partial y}\right|\ dx \le \frac{1}{\sqrt{\delta}}\tanh\frac{b-a}{2\sqrt{\delta}} < \frac{1}{\sqrt{\delta}};$$

$$\left(\int_a^b \left|\frac{\partial R(x,y)}{\partial y}\right|^2\ dx\right)^{1/2} \le \frac{1}{\sqrt{2}\sqrt[4]{\delta^3}}\sqrt{\coth\frac{b-a}{\sqrt{\delta}}} =: M_2;$$

$$\int_a^b \left|\frac{\partial R(x,y)}{\partial x}\right|\ dx \le \frac{1}{\sqrt{\delta}}\tanh\frac{b-a}{2\sqrt{\delta}} < \frac{1}{\sqrt{\delta}};$$

$$\left(\int_a^b \left|\frac{\partial R(x,y)}{\partial x}\right|^2\ dx\right)^{1/2} \le \frac{1}{\sqrt{2}\sqrt[4]{\delta^3}}\sqrt{\tanh\frac{b-a}{2\sqrt{\delta}}} < \frac{1}{\sqrt{2}\sqrt[4]{\delta^3}} =: M_3.$$

For any function $u \in W_0^\delta$, we also have

$$\|u\|_{L_\infty} \le \frac{\sqrt{\tanh \frac{b-a}{2\sqrt{\delta}}}}{\sqrt[4]{\delta}} \|u\|_{W_0^\delta} < \frac{1}{\sqrt[4]{\delta}} \|u\|_{W_0^\delta} \quad \forall u \in W_0^\delta.$$

THEOREM 3.1. *Suppose that u and U^n are the solutions of problems* (1.2) *and* (2.2)*, respectively. If $U^0 = u_0$ and u is smooth enough, then we have*

$$\max_{1 \le n \le N} \|u^n - U^n\|_{W_\infty^1} \le M \Delta t \int_0^T \{\|u_{tt}\|_{L_2} + \|u_{xxtt}\|_{L_2}\}\, dt.$$

Proof. Let $\eta^n = u^n - U^n$. By (2.1) and (2.7) we can obtain the error equation

$$\begin{aligned}
\eta^{n+1}(y) = {} & \left(1 - \frac{\mu}{\delta}\Delta t\right) \eta^n(y) - \alpha \Delta t \int_a^b \eta_x^n(x) R(x,y)\, dx \\
& + \frac{\mu}{\delta}\Delta t \int_a^b \eta^n(x) R(x,y)\, dx + \Delta t \int_a^b [\partial_t u^n(x) - u_t^n(x)] R(x,y)\, dx \\
& - \beta \Delta t \int_a^b [u^n(x) u_x^n(x) - U^n(x) U_x^n(x)] R(x,y)\, dx \\
& - \delta \Delta t \int_a^b [\partial_t u_{xx}^n(x) - u_{xxt}^n(x)] R(x,y)\, dx \quad \forall y \in [a,b].
\end{aligned} \tag{3.1}$$

By using the properties of $R(x,y)$, we have

$$\begin{aligned}
\|\eta^{n+1}\|_{L_\infty} \le {} & \left(1 + \frac{\mu}{\delta}\Delta t\right) \|\eta^n\|_{L_\infty} + \alpha \Delta t \|\eta_x^n\|_{L_\infty} + \frac{\mu}{\delta}\Delta t \|\eta^n\|_{L_\infty} \\
& + \beta \Delta t \|u^n u_x^n - U^n U_x^n\|_{L_\infty} \\
& + M_1 \Delta t \|\partial_t u^n - u_t^n\|_{L_2} + M_1 \delta \Delta t \|\partial_t u_{xx}^n - u_{xxt}^n\|_{L_2}.
\end{aligned} \tag{3.2}$$

From (3.1) we obtain

$$\begin{aligned}
\eta_y^{n+1}(y) = {} & \left(1 - \frac{\mu}{\delta}\Delta t\right) \eta_y^n(y) - \alpha \Delta t \int_a^b \eta_x^n(x) R_y(x,y)\, dx \\
& + \frac{\mu}{\delta}\Delta t \int_a^b \eta^n(x) R_y(x,y)\, dx + \Delta t \int_a^b [\partial_t u^n(x) - u_t^n(x)] R_y(x,y)\, dx \\
& - \beta \Delta t \int_a^b [u^n(x) u_x^n(x) - U^n(x) U_x^n(x)] R_y(x,y)\, dx \\
& - \delta \Delta t \int_a^b [\partial_t u_{xx}^n(x) - u_{xxt}^n(x)] R_y(x,y)\, dx.
\end{aligned}$$

Then we have

$$\begin{aligned}
\|\eta_x^{n+1}\|_{L_\infty} \le {} & \left(1 + \frac{\mu}{\delta}\Delta t\right) \|\eta_x^n\|_{L_\infty} + \frac{\alpha}{\sqrt{\delta}} \Delta t \|\eta_x^n\|_{L_\infty} + \frac{\mu}{\sqrt{\delta^3}} \Delta t \|\eta^n\|_{L_\infty} \\
& + \frac{\beta}{\sqrt{\delta}} \Delta t \|u^n u_x^n - U^n U_x^n\|_{L_\infty} \\
& + M_2 \Delta t \|\partial_t u^n - u_t^n\|_{L_2} + M_2 \delta \Delta t \|\partial_t u_{xx}^n - u_{xxt}^n\|_{L_2}.
\end{aligned} \tag{3.3}$$

In order to estimate the bound of $\|u^n u_x^n - U^n U_x^n\|_{L_\infty}$, we make the following inductional assumption:

$$\|\eta^k\|_{L_\infty} \le M_0 \quad \text{for} \quad 0 \le k \le n. \tag{3.4}$$

Since $\eta^0 = 0$, then the inductional assumption holds for $k = 0$.

We can easily show that

$$\begin{aligned}\|u^n u_x^n - U^n U_x^n\|_{L_\infty} &= \|u_x^n \eta^n + u^n \eta_x^n - \eta^n \eta_x^n\|_{L_\infty} \\ &\le \|u_x^n\|_{L_\infty}\|\eta^n\|_{L_\infty} + (\|u^n\|_{L_\infty} + M_0)\|\eta_x^n\|_{L_\infty},\end{aligned} \tag{3.5}$$

$$\|\partial_t u^n - u_t^n\|_{L_2} \le \int_{t^n}^{t^{n+1}} \|u_{tt}\|_{L_2}\, dt, \tag{3.6}$$

and

$$\|\partial_t u_{xx}^n - u_{xxt}^n\|_{L_2} \le \int_{t^n}^{t^{n+1}} \|u_{xxtt}\|_{L_2}\, dt. \tag{3.7}$$

By the assumption (3.4) and the estimates (3.2), (3.3), (3.5), (3.6), and (3.7), we obtain

$$\begin{aligned}\|\eta^{n+1}\|_{W_\infty^1} &\le (1 + M\Delta t)\|\eta^n\|_{W_\infty^1} \\ &\quad + M\Delta t \int_{t^n}^{t^{n+1}} \{\|u_{tt}\|_{L_2} + \|u_{xxtt}\|_{L_2}\}\, dt.\end{aligned}$$

By noting that $\eta^0 = 0$ and using the discrete Gronwall's inequality, we obtain

$$\|\eta^{n+1}\|_{W_\infty^1} \le M\Delta t \int_0^{t^{n+1}} (\|u_{tt}\|_{L_2} + \|u_{xxtt}\|_{L_2})\, dt. \tag{3.8}$$

It remains to check the inductional assumption when $k = n+1$. From inequality (3.8) we see that

$$\|\eta^{n+1}\|_{L_\infty} \le M\Delta t \int_0^{t^{n+1}} (\|u_{tt}\|_{L_2} + \|u_{xxtt}\|_{L_2})\, dt.$$

Then $\|\eta^{n+1}\|_{L_\infty} \le M_0$ holds by taking Δt sufficiently small. The proof is completed. ∎

THEOREM 3.2. *Suppose that u and U^n are the solutions of problems* (1.2) *and* (2.9)*, respectively. If $U^0 = u_0$ and u is smooth enough, then we have*

$$\begin{aligned}\max_{1\le n\le N} \|u^n - U^n\|_{W_\infty^1} &\le M(\Delta t)^2 \int_0^T \{\|u_{ttt}\|_{L_2} + \|u_{xxttt}\|_{L_2}\}\, dt \\ &\quad + M\Delta t \int_0^{t^1} \{\|u_{tt}\|_{L_2} + \|u_{xxtt}\|_{L_2}\}\, dt.\end{aligned}$$

Proof. Let $\eta^n = u^n - U^n$. By (2.1), (2.10), and (2.11) we can obtain the error equations

$$\begin{aligned}\eta^{n+1}(y) &= \eta^{n-1}(y) - \frac{2\mu}{\delta}\Delta t\ \eta^n(y) - 2\alpha\Delta t \int_a^b \eta_x^n(x) R(x,y)\, dx \\ &\quad + \frac{2\mu}{\delta}\Delta t \int_a^b \eta^n(x) R(x,y)\, dx + 2\Delta t \int_a^b [\bar\partial_t u^n(x) - u_t^n(x)] R(x,y)\, dx \\ &\quad - 2\beta\Delta t \int_a^b [u^n(x) u_x^n(x) - U^n(x) U_x^n(x)] R(x,y)\, dx \\ &\quad - 2\delta\Delta t \int_a^b [\bar\partial_t u_{xx}^n(x) - u_{xxt}^n(x)] R(x,y)\, dx\end{aligned} \tag{3.9}$$

and

$$\begin{aligned}\eta^1(y) &= \left(1-\frac{\mu}{\delta}\Delta t\right)\eta^0(y) - \alpha\Delta t\int_a^b \eta_x^0(x)R(x,y)\ dx\\ &\quad + \frac{\mu}{\delta}\Delta t\int_a^b \eta^0(x)R(x,y)\ dx + \Delta t\int_a^b [\partial_t u^0(x) - u_t^0(x)]R(x,y)\ dx\\ &\quad - \beta\Delta t\int_a^b [u^0(x)u_x^0(x) - U^0(x)U_x^0(x)]R(x,y)\ dx\\ &\quad - \delta\Delta t\int_a^b [\partial_t u_{xx}^0(x) - u_{xxt}^0(x)]R(x,y)\ dx. \end{aligned} \tag{3.10}$$

It follows from (3.9) and the properties of $R(x,y)$ that

$$\begin{aligned}\|\eta^{n+1}\|_{L_\infty} &\le \|\eta^{n-1}\|_{L_\infty} + \frac{2\mu}{\delta}\Delta t\ \|\eta^n\|_{L_\infty} + 2\alpha\Delta t\|\eta_x^n\|_{L_\infty} + \frac{2\mu}{\delta}\Delta t\|\eta^n\|_{L_\infty}\\ &\quad + 2\beta\Delta t\|u^n u_x^n - U^n U_x^n\|_{L_\infty}\\ &\quad + 2M_1\Delta t\|\bar\partial_t u^n - u_t^n\|_{L_2} + 2M_1\delta\Delta t\|\bar\partial_t u_{xx}^n - u_{xxt}^n\|_{L_2}. \end{aligned} \tag{3.11}$$

From (3.9) we have

$$\begin{aligned}\eta_y^{n+1}(y) &= \eta_y^{n-1}(y) - \frac{2\mu}{\delta}\Delta t\eta_y^n(y) - 2\alpha\Delta t\int_a^b \eta_x^n(x)R_y(x,y)\ dx\\ &\quad + \frac{2\mu}{\delta}\Delta t\int_a^b \eta^n(x)R_y(x,y)\ dx + 2\Delta t\int_a^b [\bar\partial_t u^n(x) - u_t^n(x)]R_y(x,y)\ dx\\ &\quad - 2\beta\Delta t\int_a^b [u^n(x)u_x^n(x) - U^n(x)U_x^n(x)]R_y(x,y)\ dx\\ &\quad - 2\delta\Delta t\int_a^b [\bar\partial_t u_{xx}^n(x) - u_{xxt}^n(x)]R_y(x,y)\ dx. \end{aligned}$$

Then

$$\begin{aligned}\|\eta_x^{n+1}\|_{L_\infty} &\le \frac{2\mu}{\delta}\Delta t\|\eta_x^n\|_{L_\infty} + \|\eta_x^{n-1}\|_{L_\infty} + \frac{2\alpha}{\sqrt{\delta}}\Delta t\|\eta_x^n\|_{L_\infty} + \frac{2\mu}{\sqrt{\delta^3}}\Delta t\|\eta_x^n\|_{L_\infty}\\ &\quad + \frac{2\beta}{\sqrt{\delta}}\Delta t\|u^n u_x^n - U^n U_x^n\|_{L_\infty}\\ &\quad + 2M_2\Delta t\|\bar\partial_t u^n - u_t^n\|_{L_2} + 2M_2\delta\Delta t\|\bar\partial_t u_{xx}^n - u_{xxt}^n\|_{L_2}. \end{aligned} \tag{3.12}$$

It is easy to show that

$$\|\bar\partial_t u^n - u_t^n\|_{L_2} \le \frac{\Delta t}{4}\int_{t^{n-1}}^{t^{n+1}} \|u_{ttt}\|_{L_2}\ dt \tag{3.13}$$

and

$$\|\bar\partial_t u_{xx}^n - u_{xxt}^n\|_{L_2} \le \frac{\Delta t}{4}\int_{t^{n-1}}^{t^{n+1}} \|u_{xxttt}\|_{L_2}\ dt. \tag{3.14}$$

By estimates (3.11), (3.12), (3.13), and (3.14) and using the same argument in the proof of Theorem 3.1, we obtain

$$\begin{aligned}\|\eta^{n+1}\|_{W_\infty^1} &\le \|\eta^{n-1}\|_{W_\infty^1} + M\Delta t\|\eta^n\|_{W_\infty^1}\\ &\quad + M(\Delta t)^2\int_{t^{n-1}}^{t^{n+1}} \{\|u_{ttt}\|_{L_2} + \|u_{xxttt}\|_{L_2}\}\ dt. \end{aligned} \tag{3.15}$$

From (3.10), we can obtain

$$\|\eta^1\|_{W_\infty^1} \le (1+M\Delta t)\|\eta^0\|_{W_\infty^1} + M\Delta t \int_0^{t^1} \{\|u_{tt}\|_{L_2} + \|u_{xxtt}\|_{L_2}\}\ dt. \tag{3.16}$$

By using the discrete Gronwall's inequality and the estimate (3.16), we can obtain the result. □

By applying similar arguments as above to full-discrete schemes, we can obtain the following error estimates.

THEOREM 3.3. *Suppose that u and U_h^n are the solutions of problems* (1.2) *and* (2.12)*, respectively. If $u_0 \in W_\infty^r$ and u is smooth enough, then we have*

$$\max_{1\le n\le N} \|u^n - U_h^n\|_{W_\infty^1} \le M\Delta t \int_0^T \{\|u_{tt}\|_{L_2} + \delta\|u_{xxtt}\|_{L_2}\}\ dt + Mh^{r-1}\|u_0\|_{W_\infty^r}.$$

THEOREM 3.4. *Suppose that u and U_h^n are the solutions of problem* (1.2) *and scheme* 4*, respectively. If $u_0 \in W_\infty^r$ and u is smooth enough, then we have*

$$\max_{1\le n\le N} \|u^n - U_h^n\|_{W_\infty^1} \le M(\Delta t)^2 \int_0^T \{\|u_{ttt}\|_{L_2} + \delta\|u_{xxttt}\|_{L_2}\}\ dt + M\Delta t \int_0^{t^1} \{\|u_{tt}\|_{L_2} + \delta\|u_{xxtt}\|_{L_2}\}\ dt + Mh^{r-1}\|u_0\|_{W_\infty^r}.$$

4. Numerical examples and results. To test the accuracy of the present method, some numerical experiments on test problems are presented in this section. We will simulate the motion of single solitary waves, the interaction of two or three solitary waves, the Maxwellian initial condition problems, and the undular bore. All experiments are done by taking parameter $\mu = 0$. Piecewise quadratic polynomial functions are employed for a basis of the finite element subspace S_h. In this case, the convergence rates of schemes 3 and 4 in the W_∞^1-error norm are $\mathcal{O}(\Delta t + h^2)$ and $\mathcal{O}((\Delta t)^2 + h^2)$, respectively.

The typical elements of the basis are defined by

$$\psi_{2k}(x) = \begin{cases} f_1\left(\dfrac{x-x_{2k}}{h}\right), & x \in [x_{2k-2}, x_{2k}], \\ f_2\left(\dfrac{x-x_{2k}}{h}\right), & x \in [x_{2k}, x_{2k+2}], \\ 0, \quad \text{otherwise}, \end{cases}$$

$$\psi_{2k+1}(x) = \begin{cases} f_3\left(\dfrac{x-x_{2k+1}}{h}\right), & x \in [x_{2k}, x_{2k+2}], \\ 0, \quad \text{otherwise}, \end{cases}$$

where $x_k = a + kh$ for $k = 0, 1, \ldots, J$, $f_1(\xi) = \frac{1}{2}(\xi+1)(\xi+2)$, $f_2(\xi) = \frac{1}{2}(\xi-1)(\xi-2)$, and $f_3(\xi) = (1-\xi)(\xi+1)$.

The accuracy of the present method will be measured by the discrete L_2-norm

$$\|u^n - U_h^n\|_{L_2} = \left(h\sum_{j=0}^{J} |u_j^n - U_{h,j}^n|^2\right)^{1/2}$$

and the discrete L_∞- and W_∞^1-norms

$$\|u^n - U_h^n\|_{L_\infty} = \max_j |u_j^n - U_{h,j}^n|,$$
$$\|u^n - U_h^n\|_{W_\infty^1} = \max\{\|u^n - U_h^n\|_{L_\infty}, \|u_x^n - (U_h^n)_x\|_{L_\infty}\}.$$

4.1. The motion of a single solitary wave. The RLW equation has an analytical solution of the form

$$u(x,t) = 3c\ \mathrm{sech}^2(k[x - x_0 - \nu t]), \tag{4.1}$$

where $\nu = 1 + \beta c$ is the wave velocity, $k = \frac{1}{2}\sqrt{\frac{\beta c}{\delta \nu}}$, and c is a constant. This solution represents the motion of a single solitary wave with amplitude $3c$ and initially centered at x_0.

It has been known that the RLW equation possesses only three invariants, which correspond to mass, momentum, and energy, respectively, and been pointed out that numerical methods that preserve some of the conserved quantities, i.e., invariants, of the given differential equations may show a more accurate behavior in time than those which do not preserve (cf. [8]). The three invariants will be checked by

$$I_1 = \int_{-\infty}^{+\infty} u\ dx \simeq h \sum_{j=0}^{J} U_{h,j}^n,$$
$$I_2 = \int_{-\infty}^{+\infty} [u^2 + \delta(u_x)^2]\ dx \simeq h \sum_{j=0}^{J} [(U_{h,j}^n)^2 + \delta(U_h^n)_{x,j}^2],$$
$$I_3 = \int_{-\infty}^{+\infty} [u^3 + 3u^2]\ dx \simeq h \sum_{j=0}^{J} [(U_{h,j}^n)^3 + 3(U_{h,j}^n)^2].$$

For the purpose of comparison with the other results of earlier works, our numerical experiments are done in the region $-40 \le x \le 60$ with parameters $c = 0.3$, 0.1, and 0.03, $x_0 = 0$, and $\alpha = \beta = \delta = 1$. Some numerical results of invariants and errors for single solitary waves with amplitude 0.3 using schemes 3 and 4 are given in Table 4.1, which shows that the second-order accurate scheme gives more accurate numerical invariants and faster convergence rate as we may expect. The convergence rates of scheme 4 in the discrete W_∞^1-norm are given in Table 4.2, in which one can see that the rates are second-order. This result could be expected by Theorem 3.4. Hence, all of the other numerical experiments are conducted by using scheme 4. Tables 4.3, 4.4, and 4.5 display the errors in the discrete L_2- and L_∞-norms and numerical values of

TABLE 4.1
Comparison of invariants and error norms for a single solitary wave with amplitude 0.3 *at* $t = 20$ *and* $-40 \le x \le 60$.

Method	h	Δt	I_1	I_2	I_3	$L_2 \times 10^4$	$L_\infty \times 10^4$
Scheme 3	0.5	0.1	3.98002	0.81387	2.59053	33.3119	12.6323
Scheme 4			3.98002	0.81049	2.57937	3.7269	1.3689
Scheme 3	0.25	0.05	3.98002	0.81225	2.58496	17.2595	6.4956
Scheme 4			3.98002	0.81047	2.57909	1.1387	0.3871
Scheme 3	0.125	0.025	3.98002	0.81137	2.58203	8.7485	3.2275
Scheme 4			3.98002	0.81046	2.57903	0.4027	0.1267
Analytic			3.97995	0.81046	2.57901		

TABLE 4.2

W^1_∞-error norm and convergence rate of scheme 4 for a single solitary wave with amplitude 0.3 at $t = 20$ and $-40 \le x \le 60$.

h	Δt	$W^1_\infty \times 10^3$	Rate
4	0.4	39.60702	
2	0.2	4.93188	3.0055
1	0.1	0.84007	2.5536
0.5	0.05	0.17773	2.2408
0.25	0.025	0.04295	2.0490

TABLE 4.3

Invariants and error norms for a single solitary wave with amplitude 0.9, $h = 0.5$, $\Delta t = 0.1$, and $-40 \le x \le 60$.

Time	I_1	I_2	I_3	$L_2 \times 10^3$	$L_\infty \times 10^3$
2	7.4939981	4.70385	16.73735	1.75364	0.90530
4	7.4939988	4.70382	16.73723	1.49070	0.87951
6	7.4939990	4.70352	16.73606	2.01436	0.96779
8	7.4939989	4.70352	16.73581	2.36221	1.05859
10	7.4939989	4.70343	16.73574	2.74597	1.21142
12	7.4939989	4.70342	16.73571	3.14852	1.30496
14	7.4939988	4.70342	16.73570	3.50652	1.40272
16	7.4939984	4.70342	16.73570	3.84006	1.55238
18	7.4939974	4.70342	16.73570	4.16757	1.69073
20	7.4939949	4.70342	16.73570	4.48006	1.77778
Analytic	7.4939976	4.70392	16.72660		

TABLE 4.4

Invariants and error norms for a single solitary wave with amplitude 0.3, $h = 0.5$, $\Delta t = 0.1$, and $-40 \le x \le 60$.

Time	I_1	I_2	I_3	$L_2 \times 10^4$	$L_\infty \times 10^4$
2	3.979945	0.810438	2.579183	1.61507	0.69463
4	3.979957	0.810510	2.579422	2.06543	0.88508
6	3.979972	0.810525	2.579470	1.87257	0.89118
8	3.979985	0.810513	2.579431	2.03264	0.93696
10	3.979998	0.810503	2.579399	2.31666	0.97767
12	3.980010	0.810498	2.579382	2.56940	1.06365
14	3.980021	0.810495	2.579374	2.85160	1.14488
16	3.980028	0.810494	2.579369	3.15012	1.21126
18	3.980029	0.810493	2.579366	3.44283	1.27663
20	3.980018	0.810493	2.579365	3.72689	1.36889
Analytic	3.979950	0.810462	2.579007		

TABLE 4.5

Invariants and error norms for a single solitary wave with amplitude 0.09, $h = 0.5$, $\Delta t = 0.1$, and $-40 \le x \le 60$.

Time	I_1	I_2	I_3	$L_2 \times 10^3$	$L_\infty \times 10^3$
2	2.107976	0.127301	0.388808	0.122311	0.115309
4	2.108708	0.127303	0.388814	0.254656	0.196527
6	2.109402	0.127305	0.388821	0.401418	0.253715
8	2.110077	0.127307	0.388825	0.556702	0.293973
10	2.110725	0.127308	0.388828	0.711371	0.322309
12	2.111318	0.127308	0.388829	0.858542	0.342251
14	2.111826	0.127308	0.388829	0.995786	0.356284
16	2.112214	0.127308	0.388829	1.124495	0.366159
18	2.112436	0.127308	0.388829	1.248279	0.373108
20	2.112426	0.127308	0.388828	1.372162	0.418654
Analytic	2.109407	0.127302	0.388806		

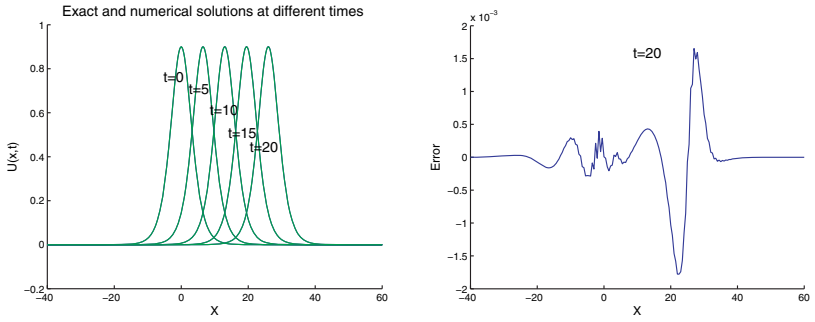

FIG. 4.1. *Exact and numerical solutions (left) and distribution of errors at* $t = 20$ *(right) for a single solitary wave with amplitude* 0.9*,* $h = 0.5$*, and* $\Delta t = 0.1$.

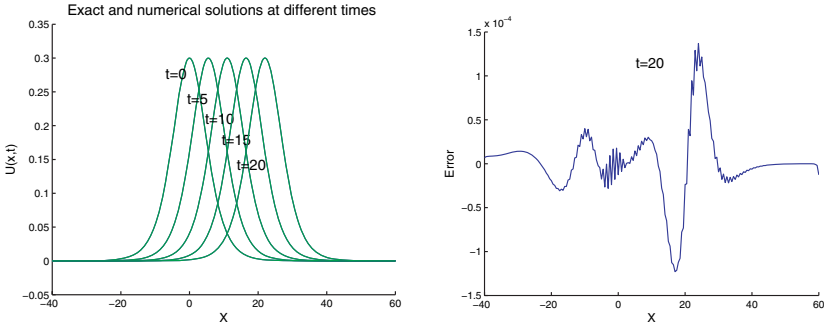

FIG. 4.2. *Exact and numerical solutions (left) and distribution of errors at* $t = 20$ *(right) for a single solitary wave with amplitude* 0.3*,* $h = 0.5$*, and* $\Delta t = 0.1$.

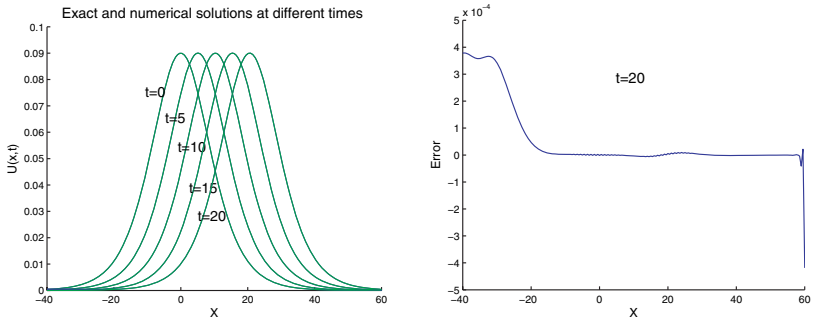

FIG. 4.3. *Exact and numerical solutions (left) and distribution of errors at* $t = 20$ *(right) for a single solitary wave with amplitude* 0.09*,* $h = 0.5$*, and* $\Delta t = 0.1$.

invariants I_1, I_2, and I_3 at different times. As we can see in these tables, the quantities of the invariants remain almost constant while the simulations are conducted up to time $t = 20$. We have simulated the motions of single solitary waves with different amplitudes. The traveling of exact and numerical waves with amplitudes 0.9, 0.3, and 0.09 are drawn in Figures 4.1, 4.2, and 4.3, respectively. The exact and numerical waves are in good agreement with each other. The distributions of differences between exact and numerical solutions are also shown in these figures.

Table 4.6 displays the invariant values and error norms obtained by the present and some previous methods, which shows that the present method provides compa-

TABLE 4.6
Comparison of invariants and error norms for a single solitary wave at $t = 20$ with $c = 0.1$, $x_0 = 0$, and $-40 \le x \le 60$.

Method	Δt	h	I_1	I_2	I_3	$L_2 \times 10^3$	$L_\infty \times 10^3$
Analytic			3.97995	0.81046	2.57901		
Present	0.1	0.5	3.98002	0.81049	2.57937	0.3727	0.1369
Present	0.05	0.5	3.98002	0.81042	2.57913	0.0796	0.0288
[3]	0.1	0.125	3.99046	0.82346	2.67399	2.157	
[4]	0.1	0.125	3.96160	0.80419	2.55829	0.0184	1.5664
[22]	0.1	0.125	3.97989	0.80925	2.57501	0.7191	0.2540
[5]QBGM1	0.1	0.125	3.97988	0.81046	2.57900	0.1922	0.0734
[5]QBGM2	0.1	0.125	3.97988	0.81046	2.57900	0.3549	0.1285
[7]	0.1	0.125	3.98206	0.81116	2.58133	0.511	0.198

rable errors and numerical invariants even if we use a larger space mesh size. The present method with larger space mesh size $h = 0.5$ and smaller time step $\Delta t = 0.05$ gives more accurate results than other methods. Since the approximate solutions can be obtained by computing vector plus matrix-vector multiplications, even though the present schemes are implicit, solving algebraic systems is not needed, and, hence, the cost of computation might be less.

4.2. The interaction of solitary waves. We first use the appropriate initial condition

$$u(x,0) = u_1 + u_2, \tag{4.2}$$

where

$$u_i = 3c_i \mathrm{sech}^2(p_i(x - x_i)), \quad c_i = 4p_i^2/(1 - 4p_i^2), \quad i = 1, 2,$$

and solve the RLW equation with parameters $\alpha = \beta = \delta = 1$. We simulate the interactions of two solitary waves having different amplitudes by taking pairs of values $(c_1, c_2) = (16/9,\ -36/11)$, $(1.7,\ -1.7)$, $(16/9,\ 9/16)$, and $(-36/11,\ -64/39)$. Figures 4.4 and 4.5 show the collisions of positive and negative waves, which produce additional solitary waves. These results are similar to the ones of Raslan [19], and these observations were confirmed by Lewis and Tjon [16]. Figures 4.6 and 4.7 show the interactions of two positive or negative solitary waves. The numerical values of invariants are displayed in Tables 4.7, 4.8, 4.9, and 4.10. They are satisfactorily close to the analytic invariant values.

Second, we consider the initial condition

$$u(x,0) = 3c_1 \mathrm{sech}^2(p_1(x - x_1)) + 3c_2 \mathrm{sech}^2(p_2(x - x_2)) + 3c_3 \mathrm{sech}^2(p_3(x - x_3))$$

to simulate the interaction of three solitary waves. In this experiment, we take $c_1 = 0.6$, $c_2 = 0.3$, $c_3 = 0.15$, $x_1 = 15$, $x_2 = 35$, and $x_3 = 60$. Figure 4.8 shows the interaction of the three solitary waves. The numerical invariant values are given in Table 4.11, and these values are sufficiently close to analytic ones.

4.3. The Maxwellian initial condition. We consider the numerical solution of the RLW equation with the Maxwellian initial condition

$$u(x,0) = \exp(-(x - 7)^2) \tag{4.3}$$

and boundary conditions

$$u(a,t) = u(b,t) = 0.$$

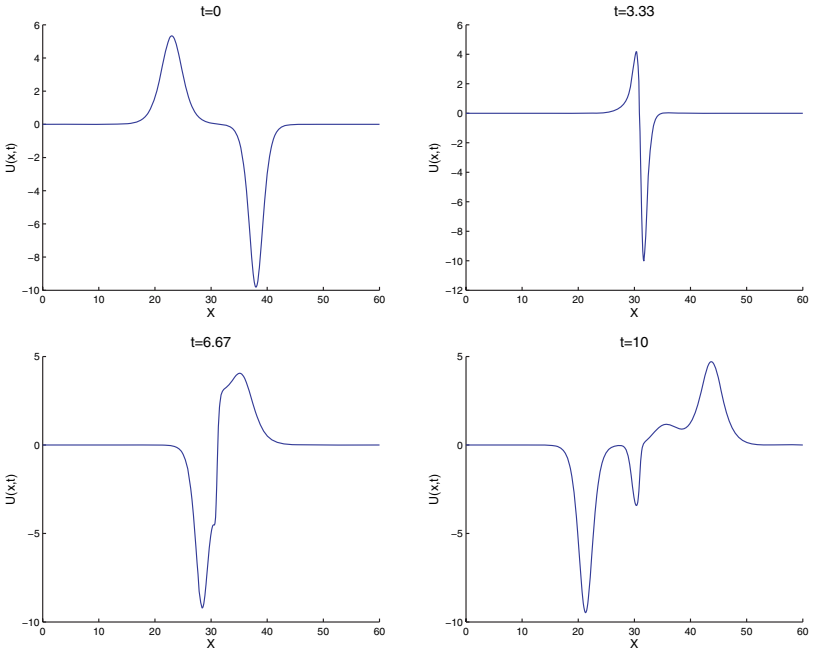

FIG. 4.4. *Interaction of two solitary waves for* $c_1 = 16/9$, $c_2 = -36/11$, $h = 0.1$, *and* $\Delta t = 0.01$.

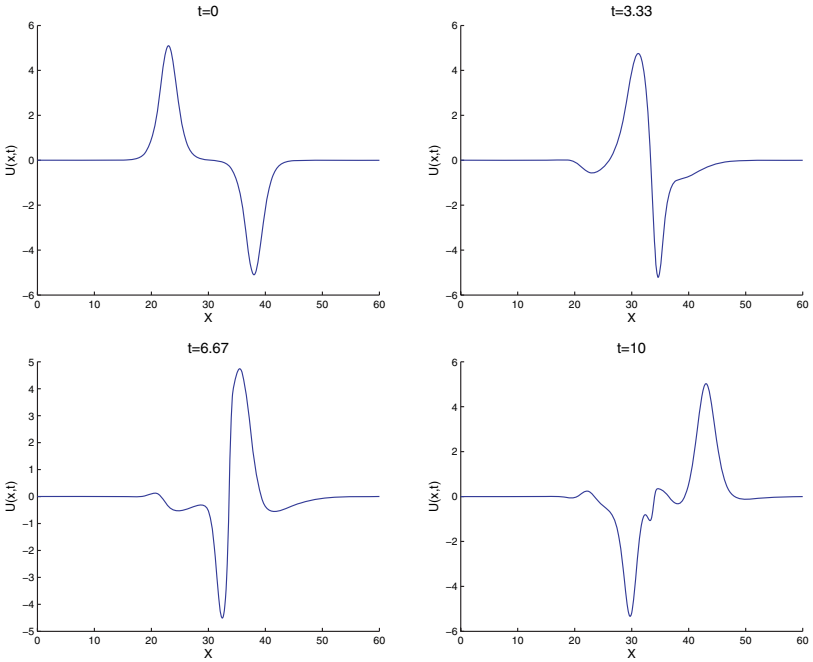

FIG. 4.5. *Interaction of two solitary waves for* $c_1 = 1.7$, $c_2 = -1.7$, $h = 0.1$, *and* $\Delta t = 0.01$.

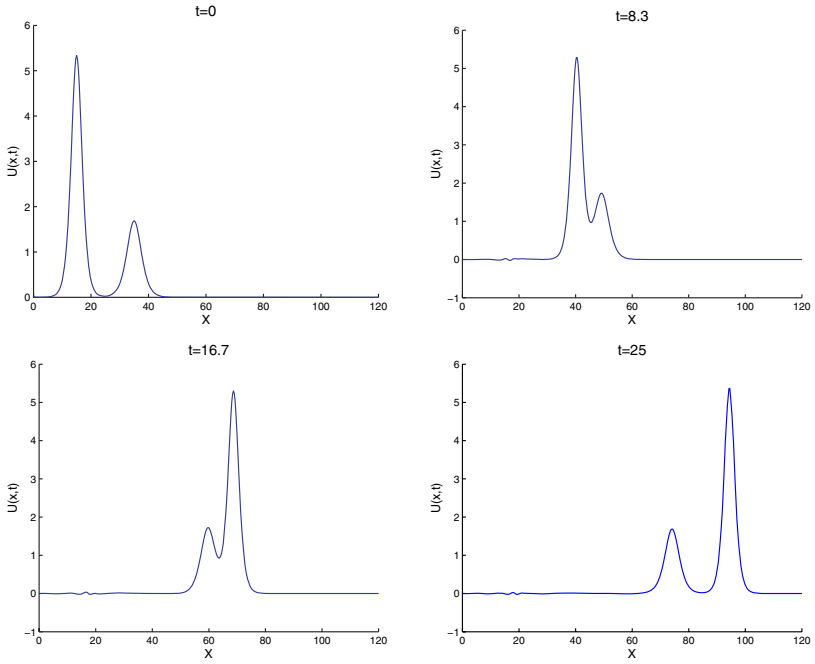

FIG. 4.6. *Interaction of two solitary waves for* $c_1 = 16/9$, $c_2 = 9/16$, $h = 0.3$, *and* $\Delta t = 0.1$.

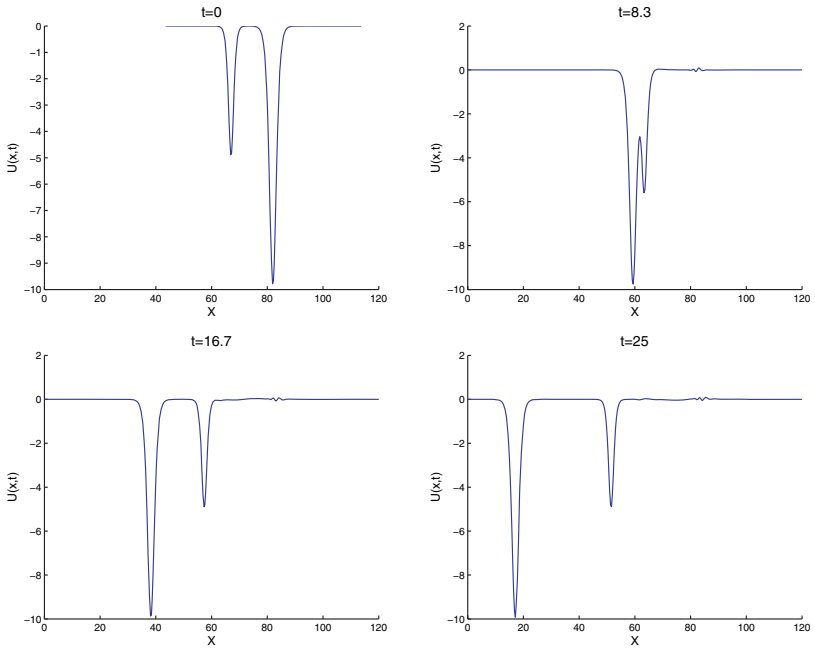

FIG. 4.7. *Interaction of two solitary waves for* $c_1 = -36/11$, $c_2 = -64/39$, $h = 0.3$, *and* $\Delta t = 0.1$.

TABLE 4.7
Invariants of two solitary waves for $c_1 = 16/9$, $c_2 = -36/11$, $h = 0.1$, and $\Delta t = 0.01$.

Time	I_1	I_2	I_3
2	−6.060606	382.618153	−351.032096
4	−6.060607	371.185311	−351.189412
6	−6.060617	378.636541	−351.112271
8	−6.060619	381.873891	−350.997216
10	−6.060755	382.301648	−351.023238
Analytic	−6.060606	382.859871	−350.928198

TABLE 4.8
Invariants of two solitary waves for $c_1 = 1.7$, $c_2 = -1.7$, $h = 0.1$, and $\Delta t = 0.01$.

Time	I_1	I_2	I_3
2	0.0000045	166.38360	416.18365
4	0.0000760	165.62517	416.18684
6	0.0005786	164.67011	416.25369
8	0.0028347	166.25189	416.18794
10	0.0102995	166.30703	416.18728
Analytic	0	166.46400	416.16000

TABLE 4.9
Invariants of two solitary waves for $c_1 = 16/9$, $c_2 = 9/16$, $h = 0.3$, and $\Delta t = 0.1$.

Time	I_1	I_2	I_3
2	37.916929	121.079520	750.135884
4	37.917363	121.095127	750.242027
6	37.918248	121.061588	749.980504
8	37.919569	121.039125	749.883906
10	37.920769	120.914761	748.968489
12	37.920806	120.741106	747.517011
14	37.918837	120.817004	748.176802
16	37.915194	120.991542	749.543660
18	37.911734	121.065459	750.046070
20	37.910891	121.084495	750.164600
22	37.913804	121.090289	750.192271
24	37.918999	121.091116	750.197670
25	37.913593	121.091584	750.198886
Analytic	37.916667	120.518611	744.042342

TABLE 4.10
Invariants of two solitary waves for $c_1 = -36/11$, $c_2 = -64/39$, $h = 0.3$, and $\Delta t = 0.1$.

Time	I_1	I_2	I_3
3	−45.035040	337.680275	−1102.432673
6	−45.035027	336.951084	−1099.963635
9	−45.035036	337.448777	−1101.952270
12	−45.035032	337.770072	−1102.421010
15	−45.035046	337.692270	−1102.442376
18	−45.035051	337.697795	−1102.441761
21	−45.035038	337.696489	−1102.440516
24	−45.034953	337.696638	−1102.442441
25	−45.034872	337.694856	−1102.443743
Analytic	−45.034965	336.985210	−1077.824516

Computations are done for $\delta = 0.04$, 0.01, and 0.001. The numerical invariants are given in Table 4.12, which shows that they are satisfactorily close to the initial values during the simulations. The numerical solution curves for different values of δ, are

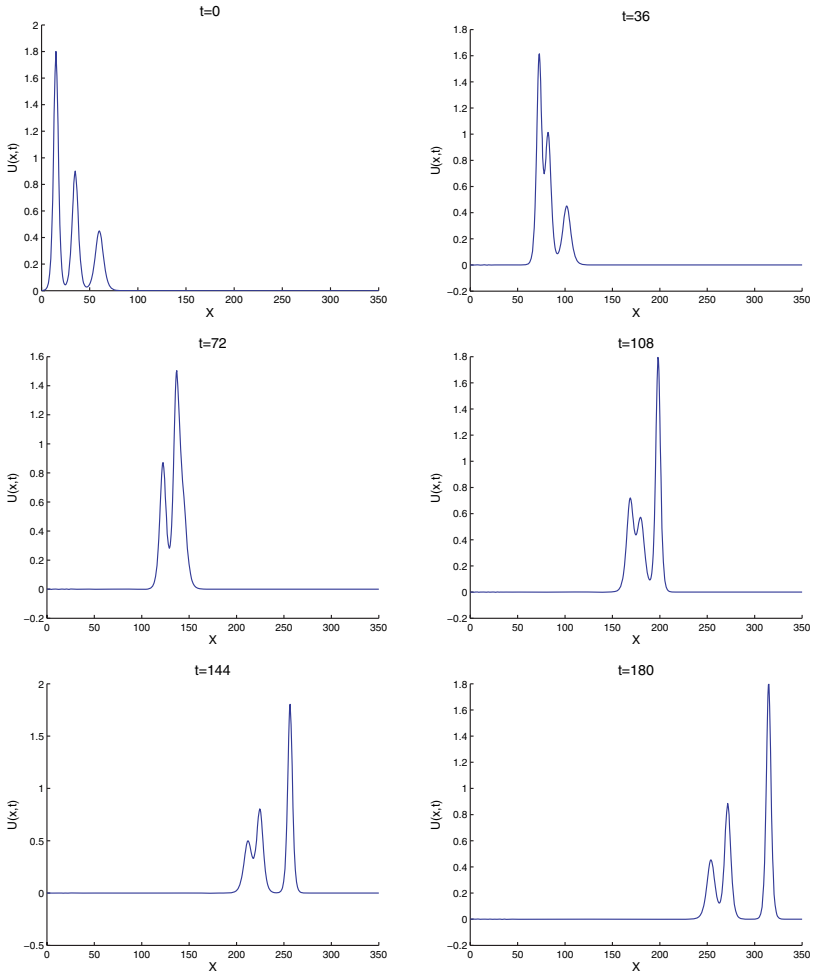

FIG. 4.8. *Interaction of three solitary waves for* $c_1 = 0.6$, $c_2 = 0.3$, $c_3 = 0.15$, $h = 0.5$, *and* $\Delta t = 0.1$.

TABLE 4.11
Invariants for three solitary waves for $c_1 = 0.6$, $c_2 = 0.3$, $c_3 = 0.15$, $h = 0.5$, *and* $\Delta t = 0.1$.

Time	I_1	I_2	I_3
20	24.23657	21.42319	84.59869
40	24.23697	21.42495	84.56117
60	24.23747	21.42381	84.57375
80	24.23744	21.43070	84.55262
100	24.23675	21.42443	84.59660
120	24.23577	21.42480	84.60136
140	24.23324	21.42468	84.60314
160	24.23293	21.42457	84.60525
180	24.24387	21.42461	84.60649
Analytic	24.23552	21.40536	84.39468

TABLE 4.12
Invariants for the Maxwellian initial condition with $h = 0.1$ and $\Delta t = 0.01$.

δ	Time	I_1	I_2	I_3
0.04	0	1.772454	1.303446	4.783268
	2	1.772454	1.302727	4.784430
	4	1.772456	1.302688	4.784503
	6	1.772466	1.302701	4.784515
	8	1.772440	1.302707	4.784517
	10	1.772458	1.302708	4.784515
	12	1.772445	1.302709	4.784516
0.01	0	1.772454	1.265847	4.783268
	2	1.772462	1.264875	4.789392
	4	1.772469	1.263882	4.795030
	6	1.772494	1.263853	4.796123
	8	1.772422	1.263861	4.796357
0.001	0	1.772454	1.254567	4.783268
	1	1.772509	1.255505	4.789821
	2	1.772428	1.254533	4.842533
	3	1.772135	1.250175	4.863419
	4	1.772700	1.260545	4.929862

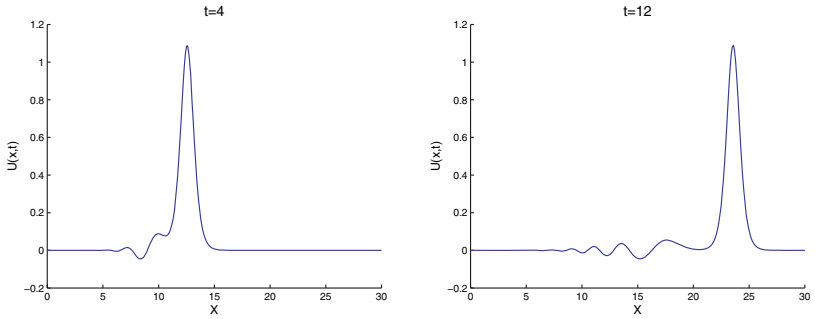

FIG. 4.9. *Numerical solution curves at $t = 4$ and 12 for the Maxwellian initial condition, $\delta = 0.04$, $h = 0.1$, and $\Delta t = 0.01$.*

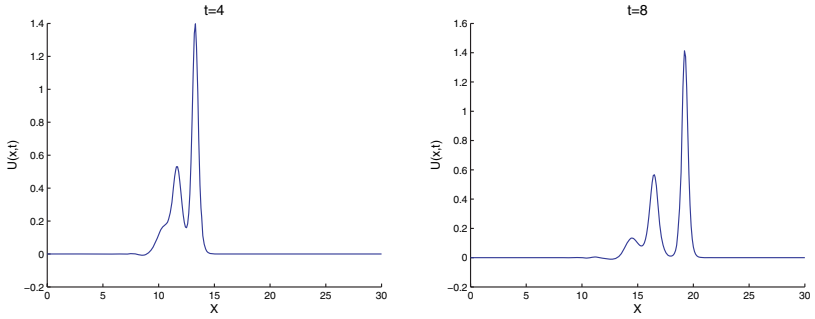

FIG. 4.10. *Numerical solution curves at $t = 4$ and 8 for the Maxwellian initial condition, $\delta = 0.01$, $h = 0.1$, and $\Delta t = 0.01$.*

drawn in Figures 4.9, 4.10, and 4.11. The number of the solitary waves depends on the value of δ, and choosing smaller δ produces more solitary waves. This result accords with the ones that are presented in [12, 19].

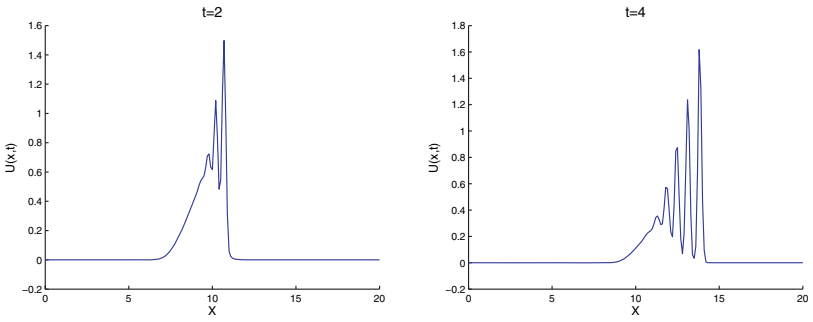

FIG. 4.11. *Numerical solutions at $t = 2$ and 4 for the Maxwellian initial condition, $\delta = 0.001$, $h = 0.1$, and $\Delta t = 0.01$.*

4.4. The development of an undular bore. As our last experiment, we simulate the development of an undular bore. For that purpose, we consider the RLW equation with the physical boundary conditions $u(x,t) \to U_0$ as $x \to -\infty$ and $u(x,t) \to 0$ as $x \to +\infty$ and the initial condition (cf. [2, 9, 21])

$$u(x,0) = \frac{U_0}{2}\left[1 - \tanh\left\{\frac{x - x_0}{d}\right\}\right],$$

where $u(x,0)$ denotes the elevation of the water surface above the equilibrium level at time $t = 0$. U_0 represents the magnitude of the change in water level which is centered at x_0, and d measures the steepness of the change. In our numerical experiments, all computations are done with parameters $\alpha = 1$, $\beta = 3/2$, $\delta = 1/6$, $U_0 = 0.1$, $x_0 = 0$, $h = 0.5$, $\Delta t = 0.1$, and $d = 2$, 5 over the region $-20 \le x \le 300$. The boundary conditions we used are $u(-20,t) = 0.1$ and $u(300,t) = 0$.

For nonhomogeneous Dirichlet boundary condition problems, the explicit formulas of scheme 4 for numerical solutions are slightly different from (2.13) and (2.14). In this case, the numerical solution U_h^n can be written as

$$U_h^n(x) =: U_0\psi_0(x) + \tilde{U}_h^n(x),$$

where $\tilde{U}_h^n \in S_h \subset H_0^1$ and

$$\psi_0(x) = \begin{cases} f_2\left(\dfrac{x - x_0}{h}\right), & x \in [x_0, x_2], \\ 0, \quad \text{otherwise.} \end{cases}$$

Then we have the explicit formulas

$$\begin{aligned}\tilde{U}_h^{n+1}(y) = \tilde{U}_h^{n-1}(y) &- 2\Delta t\frac{\mu}{\delta}\tilde{U}_h^n(y) - 2U_0\Delta t\frac{\mu}{\delta}\int_a^b \psi_0(x)R(x,y)\,dx \\ &-2U_0\Delta t\mu\int_a^b (\psi_0)_x(x)R_x(x,y)\,dx \\ &- 2\Delta t\int_a^b \left\{\alpha(U_h)_x^n(x) - \frac{\mu}{\delta}U_h^n(x)\right\}R(x,y)\,dx \\ &- 2\beta\Delta t\int_a^b U_h^n(x)(U_h)_x^n(x)R(x,y)\,dx \quad \forall y \in [a,b]\end{aligned}$$

TABLE 4.13
Numerical invariants for $d = 2$ with $h = 0.5$ and $\Delta t = 0.1$.

Time	M_1	M_2	M_3
25	0.107528	0.011006	0.034119
50	0.107500	0.011001	0.034100
75	0.107494	0.011000	0.034095
100	0.107508	0.011002	0.034103
125	0.107493	0.010999	0.034093
150	0.107508	0.011002	0.034102
175	0.107494	0.011000	0.034093
200	0.107505	0.011002	0.034100
225	0.107497	0.011000	0.034095
250	0.107381	0.011001	0.034098
Analytic	0.107500	0.011000	0.034113

and

$$\begin{aligned}\tilde{U}_h^1(y) = &\left(1 - \Delta t\frac{\mu}{\delta}\right)\tilde{U}_h^0(y) - U_0\Delta t\frac{\mu}{\delta}\int_a^b \psi_0(x)R(x,y)\ dx\\ &-U_0\Delta t\mu\int_a^b (\psi_0)_x(x)R_x(x,y)\ dx\\ &-\Delta t\int_a^b \left\{\alpha(U_h)_x^0(x) - \frac{\mu}{\delta}U_h^0(x)\right\}R(x,y)\ dx\\ &-\ \beta\Delta t\int_a^b U_h^0(x)(U_h)_x^0(x)R(x,y)\ dx \quad \forall y \in [a,b].\end{aligned}$$

Under the above physical boundary conditions the invariants I_1, I_2, and I_3 are not constant but increase linearly at the following rates [9]:

$$M_1 = \frac{dI_1}{dt} = \frac{d}{dt}\int_{-\infty}^{+\infty} u(x,t)\ dx = U_0 + \frac{\beta}{2}U_0^2 = 0.1075,$$

$$M_2 = \frac{dI_2}{dt} = \frac{d}{dt}\int_{-\infty}^{+\infty} (u^2(x,t) + \delta u_x^2(x,t))\ dx = U_0^2 + \frac{2\beta}{3}U_0^3 = 0.011,$$

$$\begin{aligned}M_3 = \frac{dI_3}{dt} &= \frac{d}{dt}\int_{-\infty}^{+\infty} \left(3u^2(x,t) + u^3(x,t)\right)\ dx\\ &= 3U_0^2 + (1+2\beta)U_0^3 + \frac{3\beta}{4}U_0^4 = 0.0341125.\end{aligned}$$

In our experiments, the numerical values of invariants M_1, M_2, and M_3 are computed by using the backward difference quotients $M_i(t^n) = (I_i(t^n) - I_i(t^{n-1}))/\Delta t$ for $i = 1, 2, 3$ and are displayed in Tables 4.13 and 4.14. They are sufficiently close to the analytic ones. Figures 4.12 and 4.13 illustrate the undular bore profiles at $t = 100$ and 250 on the interval $[0, 300]$ for $d = 2$ and 5. These results are similar to those given in [9].

TABLE 4.14
Numerical invariants for $d = 5$ with $h = 0.5$ and $\Delta t = 0.1$.

Time	M_1	M_2	M_3
25	0.107463	0.010993	0.034084
50	0.107523	0.011005	0.034119
75	0.107483	0.010997	0.034091
100	0.107513	0.011003	0.034108
125	0.107490	0.010999	0.034092
150	0.107508	0.011002	0.034103
175	0.107495	0.011000	0.034094
200	0.107504	0.011001	0.034099
225	0.107499	0.011000	0.034096
250	0.107282	0.011001	0.034097
Analytic	0.107500	0.011000	0.034113

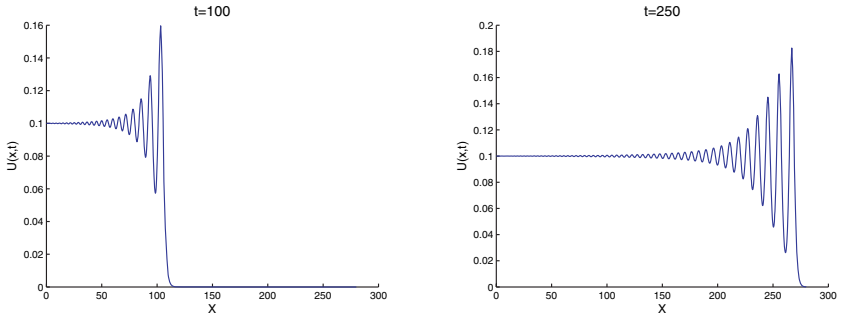

FIG. 4.12. *Numerical solution profiles of the undular bore at $t = 100$ and 250 for $d = 2$ with $h = 0.5$ and $\Delta t = 0.1$.*

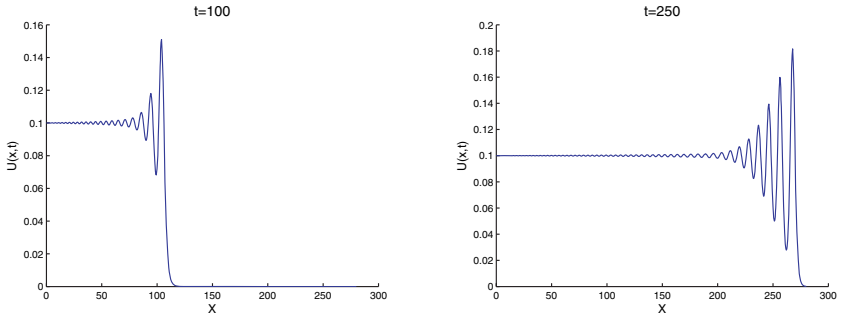

FIG. 4.13. *Numerical solution profiles of the undular bore at $t = 100$ and 250 for $d = 5$ with $h = 0.5$ and $\Delta t = 0.1$.*

5. Conclusion. A numerical method by using a reproducing kernel function is devised and analyzed. The performance of this method was examined on four test examples by using piecewise quadratic polynomial basis functions. In our numerical experiments, the error norms are satisfactorily small and the numerical invariant values are almost kept constantly. This method successfully simulates the motion of single solitary waves with different amplitudes, interaction of two or three solitary waves, development of solitary waves generated by using the Maxwellian initial condition, and development of an undular bore. Based on our numerical experiments, we may say that the present method is a practical and competitive numerical technique.

Acknowledgments. The authors thank the anonymous referees for helpful comments and suggestions on this paper.

REFERENCES

[1] Z. Aronszajn, *Theory of reproducing kernels*, Trans. Amer. Math. Soc., 68 (1950), pp. 337–404.
[2] D. Bhardwaj and R. Shankar, *A computational method for regularized long wave equation*, Comput. Math. Appl., 40 (2000), pp. 1397–1404.
[3] I. Dağ, *Least-square quadratic B-spline finite element method for the regularized long wave equation*, Comput. Methods Appl. Mech. Engrg., 182 (2000), pp. 205–215.
[4] I. Dağ and M. N. Özer, *Approximation of the RLW equation by the least square cubic B-spline finite element method*, Appl. Math. Model., 25 (2001), pp. 221–231.
[5] I. Dağ, B. Saka, and D. Irk, *Galerkin method for the numerical solution of the RLW equation using quintic B-splines*, J. Comput. Appl. Math., 190 (2006), pp. 532–547.
[6] K. Djidjeli, W. G. Price, E. H. Twizell, and Q. Cao, *A linearized implicit pseudo-spectral method for some model equations: The regularized long wave equations*, Comm. Numer. Methods Engrg., 19 (2003), pp. 847–863.
[7] A. Dogan, *Numerical solution of RLW equation using linear finite elements within Galerkin's method*, Appl. Math. Model., 26 (2002), pp. 771–783.
[8] A. Durán and M. A. Lopez-Marcos, *Conservative numerical methods for solitary wave interactions*, J. Phys. A, 36 (2003), pp. 7761–7770.
[9] A. Esen and S. Kutluay, *Application of a lumped Galerkin method to the regularized long wave equation*, Appl. Math. Comput., 174 (2006), pp. 833–845.
[10] J. C. Eilbeck and G. R. McGuire, *Numerical study of the RLW equation* I, J. Comput. Phys., 19 (1975), pp. 43–57.
[11] J. C. Eilbeck and G. R. McGuire, *Numerical study of the RLW equation* II, J. Comput. Phys., 23 (1977), pp. 63–73.
[12] L. R. T. Gardner and G. A. Gardner, *Solitary waves of the regularized long wave equation*, J. Comput. Phys., 91 (1990), pp. 441–459.
[13] L. R. T. Gardner, G. A. Gardner, and I. Dag, *A B-spline finite element method for the regularized long wave equation*, Comm. Numer. Methods Engrg., 11 (1995), pp. 59–68.
[14] B. Guo and V. S. Manoranjan, *A spectral method for solving the RLW equation*, IMA J. Numer. Anal., 5 (1985), pp. 307–318.
[15] P. C. Jain and L. Iskandar, *Numerical solution of the RLW equation*, Comput. Methods Appl. Mech. Engrg., 20 (1979), pp. 195–200.
[16] J. C. Lewis and J. A. Tjon, *Resonant production of solutions in the RLW equation*, Phys. Lett., 73A (1979), pp. 275–279.
[17] D. H. Peregrine, *Calculations of the development of an undular bore*, J. Fluid Mech., 25 (1966), pp. 321–330.
[18] J. I. Ramos, *Explicit finite difference methods for the EW and RLW equations*, Appl. Math. Comput., 179 (2007), pp. 622–638.
[19] K. R. Raslan, *A computational method for the regularized long wave (RLW) equation*, Appl. Math. Comput., 167 (2005), pp. 1101–1118.
[20] S. Xie, *Optimal approximation and applications in some spaces with RKF*, Appl. Math. J. Chinese Univ. Ser. A, 11 (1996), pp. 83–90.
[21] S. I. Zaki, *A least-squares finite element scheme for the EW equation*, Comput. Methods Appl. Mech. Engrg., 169 (2000), pp. 587–594.
[22] S. I. Zaki, *Solitary waves of the splitted RLW Equation*, Comput. Phys. Comm., 138 (2001), pp. 80–91.